

# Pharmacokinetic-pharmacodynamic correlation from mouse to human with pazopanib, a multikinase angiogenesis inhibitor with potent antitumor and antiangiogenic activity

Rakesh Kumar, Victoria B. Knick, Sharon K. Rudolph, Jennifer H. Johnson, Renae M. Crosby, Ming-Chih Crouthamel, Teresa M. Hopper, Charles G. Miller, Laura E. Harrington, James A. Onori, Robert J. Mullin, Tona M. Gilmer, Anne T. Truesdale, Andrea H. Epperly, Amogh Bloor, Jeffrey A. Stafford, Deirdre K. Luttrell, and Mui Cheung

GlaxoSmithKline, Collegeville, Pennsylvania

## Abstract

With the development of targeted therapeutics, especially for small-molecule inhibitors, it is important to understand whether the observed *in vivo* efficacy correlates with the modulation of desired/intended target *in vivo*. We have developed a small-molecule inhibitor of all three vascular endothelial growth factor (VEGF) receptors (VEGFR), platelet-derived growth factor receptor, and c-Kit tyrosine kinases, pazopanib (GW786034), which selectively inhibits VEGF-induced endothelial cell proliferation. It has good oral exposure and inhibits angiogenesis and tumor growth in mice. Because bolus administration of the compound results in large differences in  $C_{max}$  and  $C_{trough}$ , we investigated the effect of continuous infusion of a VEGFR inhibitor on tumor growth and angiogenesis. GW771806, which has similar enzyme and cellular profiles to GW786034, was used for these studies due to higher solubility requirements for infusion studies. Comparing the pharmacokinetics by two different routes of administration (bolus p.o. dosing and continuous infusion), we showed that the antitumor and antiangiogenic activity of VEGFR inhibitors is dependent on steady-state concentration of the compound above a threshold. The steady-state

concentration required for these effects is consistent with the concentration required for the inhibition of VEGF-induced VEGFR2 phosphorylation in mouse lungs. Furthermore, the steady-state concentration of pazopanib determined from preclinical activity showed a strong correlation with the pharmacodynamic effects and antitumor activity in the phase I clinical trial. [Mol Cancer Ther 2007;6(7):2012–21]

## Introduction

Tumor angiogenesis is one of the hallmarks of cancer and an attribute of all types of human tumors (1). Angiogenesis is not an intrinsic characteristic of tumor cells, but is initiated by proangiogenic factors like vascular endothelial growth factor (VEGF), platelet-derived growth factor (PDGF), fibroblast growth factor (FGF), angiopoietins, etc., which act by binding to tyrosine kinase receptors on endothelial and other stromal cells (2). VEGF is expressed by various tumor and host cells and is up-regulated in the tumor microenvironment (3). Members of the VEGF family (VEGF-A, VEGF-B, VEGF-C, and VEGF-D) bind to the corresponding receptor tyrosine kinases [VEGF receptor (VEGFR)-1 (Flt-1), VEGFR2 (Flk-1, KDR), and VEGFR3 (Flt-4)]. VEGFR2 is the primary tyrosine kinase receptor mediating downstream events such as vascular permeability, endothelial cell proliferation, invasion, migration, and survival (4–6). Other receptors, such as PDGF receptors (PDGFR $\alpha$  and PDGFR $\beta$ ), are expressed on multiple cell types, including pericytes and smooth muscle cells, and regulate pericyte differentiation and vascular survival (7). PDGFR is also implicated to provide an autocrine growth and survival signal in certain tumor cells (e.g., by overexpression in glioma, activating mutations in dermatofibrosarcoma protuberans and a subset of gastrointestinal stromal tumors, or activating translocation in chronic myelogenous monocytic leukemia; ref. 8). Stem cell factor receptor (Kit) is expressed on primitive hematopoietic cells, melanocytes, and germ cells and has been implicated in the pathogenesis of several human malignancies, including gastrointestinal stromal tumor, melanoma, small-cell lung cancer, and ovarian and breast carcinomas (9).

Recognition of the VEGF pathway as a key regulator of angiogenesis has led to the development of several therapeutic approaches, including antibodies against the VEGF ligand or VEGFR2 receptor as well as multiple small-molecule inhibitors of VEGFRs (10). Several of these agents have shown promising clinical activity either as a single agent or in combination with existing therapies against a variety of tumor types. Bevacizumab, a monoclonal

Received 3/20/07; revised 5/14/07; accepted 5/25/07.

The costs of publication of this article were defrayed in part by the payment of page charges. This article must therefore be hereby marked *advertisement* in accordance with 18 U.S.C. Section 1734 solely to indicate this fact.

**Note:** All authors are present or former employees of GlaxoSmithKline.

**Requests for reprints:** Rakesh Kumar, Oncology Biology, 1250 South Collegeville Road, UP1450, Collegeville, PA 19426. Phone: 610-917-4855; Fax: 610-917-4181. E-mail: rakesh.2.kumar@gsk.com

Copyright © 2007 American Association for Cancer Research.

doi:10.1158/1535-7163.MCT-07-0193

antibody that selectively targets VEGF-A, is approved for first- or second-line therapy in patients with metastatic colorectal cancer (11) and first-line therapy in non-small-cell lung cancer (12). Sunitinib, a multitargeted tyrosine kinase inhibitor, is approved for treatment in patients with renal cell carcinoma and gastrointestinal stromal tumor (13, 14). Sorafenib, an inhibitor of Raf kinase as well as VEGFRs, was approved for treatment of advanced renal cell carcinoma (15).

The present study describes an orally bioavailable, ATP-competitive, multitargeted kinase inhibitor, pazopanib (GW786034), and the drug concentration requirement for maximal *in vivo* activity. Pazopanib is a low nanomolar inhibitor of VEGFR, PDGFR, and c-Kit tyrosine kinases. It inhibits angiogenesis and the growth of a broad range of human tumor xenografts in mice. We also describe the pharmacokinetic-pharmacodynamic relationship of the VEGFR inhibitor for maximal *in vivo* activity and show that the drug concentration required for inhibition of angiogenesis and tumor growth in preclinical models can be used to guide dose selection for clinical studies.

## Materials and Methods

### Pazopanib Preparation

Pazopanib (GW786034) is a novel 2*H*-indazolylpyrimidine compound [5-({4-[2,3-dimethyl-2*H*-indazole-6-yl]methylamino}2-pyrimidinyl)amino)-2-methylbenzenesulfonamide]. It was synthesized at GlaxoSmithKline. For proliferation, phosphorylation, and enzyme phosphorylation studies, pazopanib was obtained in a purified powder and reconstituted in DMSO at a concentration of 10 mmol/L before use. For the tumor xenograft, pharmacodynamic studies, and the Matrigel plug assay, pazopanib was formulated in aqueous 0.5% hydroxypropylmethylcellulose and 0.1% Tween 80.

Studies requiring parenteral administration of the VEGFR inhibitor used GW771806. GW771806 has similar enzyme and cellular profiles to pazopanib (Supplementary Tables S1 and S2),<sup>1</sup> but with improved solubility, which allowed for the preparation of a parenteral dosage form.

### Animals

Female Swiss nude mice were obtained from Taconic and C.B-17 severe combined immunodeficient mice were obtained from Charles River. All animal studies were done in compliance with federal requirements, GlaxoSmithKline policy on the Care and Use of Animals, and with related codes of practice.

### Kinase Assays

The ability of pazopanib (mono-HCl and free base) to inhibit the activity of a wide variety of kinases was tested *in vitro*. VEGFR enzyme assays for VEGFR1, VEGFR2 (human, dog, mouse, and rat), and VEGFR3 were run in homogeneous time-resolved fluorescence (HTRF) format

in 384-well microtiter plates using a purified, baculovirus-expressed glutathione *S*-transferase-fusion protein encoding the catalytic COOH terminus of human VEGFR kinase 1, 2, or 3. For VEGFR2, reactions were initiated by the addition of 10  $\mu$ L of activated VEGFR2 kinase solution [final concentration, 1 nmol/L enzyme in 0.1 mol/L HEPES (pH 7.5) containing 0.1 mg/mL bovine serum albumin, 300  $\mu$ mol/L DTT] to 10- $\mu$ L substrate solution [final concentration, 360 nmol/L peptide (biotin-aminohexyl-EEEEY-FELVAKKKK-NH<sub>2</sub>), 75  $\mu$ mol/L ATP, 10  $\mu$ mol/L MgCl<sub>2</sub>] and 1  $\mu$ L of titrated compound in DMSO. Plates were incubated at room temperature for 60 min, then the reaction was quenched by the addition of 20- $\mu$ L 100 mmol/L EDTA. After quenching, 20- $\mu$ L HTRF reagents (final concentration, 15 nmol/L streptavidin-linked allophycocyanin (Perkin-Elmer), 1 nmol/L europium-labeled anti-phosphotyrosine antibody (Perkin-Elmer) diluted in 0.1 mg/mL bovine serum albumin, 0.1 mol/L HEPES (pH 7.5)) were added and the plates incubated for a minimum of 10 min before reading. The fluorescence at 665 nm was measured with a Wallac Victor plate reader using a time delay of 50  $\mu$ s. Similar protocols were followed for VEGFR1 and VEGFR3.

Pazopanib inhibition of a number of kinases outside of the VEGFR family was also determined. These included Abl1; Akt3; activin-like kinase 6; cyclin-dependent kinase 1/cyclin A; cyclin-dependent kinase 2/cyclin A; c-fms; c-Kit; epidermal growth factor receptor; ErbB2; ErbB4; EphB4; focal adhesion kinase; FGF receptors (FGFR) 1, 2, and 3; Flt-3; glycogen synthase kinase 3; insulin-like growth factor type I receptor; insulin receptor; interleukin-2-inducible T-cell kinase; c-jun NH<sub>2</sub>-terminal kinases 1, 2, and 3; lymphocyte-specific protein tyrosine kinase (murine); Met; p38 $\alpha$ ; PDGFR $\alpha$  and PDGFR $\beta$ ; protein kinase C- $\beta$ 1 and - $\beta$ 2; polo-like kinases 1 and 3; Ret; Src; Syk; Tie-2; and Wee1. All assays were conducted using purified, recombinantly expressed catalytic domains of the kinases. Assays were conducted using ATP concentrations below the enzyme  $K_{m,app}$  and kinase-specific biotinylated peptides. The detection system for various kinase assays was either HTRF or scintillation proximity assay.

The data for dose responses were plotted as percent inhibition calculated with the data reduction formula  $100 \times [1 - (U_1 - C_2) / (C_1 - C_2)]$  versus concentration of compound, where  $U$  is the unknown value,  $C_1$  is the average control value obtained for 1- $\mu$ L DMSO, and  $C_2$  is the average control value obtained for 0.035 mol/L EDTA. Inhibition curves were generated by plotting percentage control activity versus log<sub>10</sub> of the concentration of each kinase. The IC<sub>50</sub> values were calculated by nonlinear regression. Data were fitted with a curve described as follows:  $y = [(V_{max} \cdot x) / (K + x)] + Y_2$ , where  $V_{max}$  is the upper asymptote,  $Y_2$  is the  $Y$  intercept, and  $K$  is the IC<sub>50</sub>.

### Proliferation Assays Using Human Umbilical Vascular Endothelial Cell Cultures

The effect of kinase inhibitors on cell proliferation was measured using the bromodeoxyuridine (BrdUrd) incorporation method using commercially available kits (Roche

<sup>1</sup> Supplementary material for this article is available at Molecular Cancer Therapeutics Online (<http://mct.aacrjournals.org/>).

Diagnostics). Briefly, human umbilical vascular endothelial cells (HUVEC; Clonetics) were seeded in medium containing 5% fetal bovine serum in type 1 collagen-coated 96-well plates and incubated overnight at 37°C, 5% CO<sub>2</sub>. The medium was aspirated from the cells, and various concentrations of pazopanib in serum-free medium were added to each well. After 30 min, VEGF (10 ng/mL) or basic FGF (bFGF; 0.3 ng/mL) was added to the wells. Cells were incubated for an additional 72 h and BrdUrd (10 μmol/L) was added during the last 18 to 24 h of incubation. At the end of incubation, BrdUrd incorporation in cells was measured by ELISA according to the manufacturer's instructions. Data were fitted with a curve described by the equation  $y = V_{\max} \cdot \{1 - [x / (K + x)]\}$ , where  $K$  is equal to the IC<sub>50</sub>.

To assess human foreskin fibroblast and tumor cell proliferation, cells were plated in culture medium containing 10% fetal bovine serum and incubated overnight at 37°C, 5% CO<sub>2</sub>. Different concentrations of pazopanib in serum-free medium were added to each well to achieve a final concentration of 0.3% (v/v) DMSO and 5% fetal bovine serum. Cells were incubated for 72 h at 37°C, 10% CO<sub>2</sub>. BrdUrd (10 μmol/L final concentration) was added either 1.5 or 18 h before termination for tumor cells and human foreskin fibroblasts, respectively.

#### Receptor Phosphorylation Assays

Phosphorylation of VEGFR2 was assessed in HUVEC stimulated with VEGF. HUVEC were plated in type I collagen-coated 10-cm plates in Clonetics EGM-MV medium (Clonetics) at  $1.0 \times 10^6$  to  $1.5 \times 10^6$  per plate. After 24 h, the confluent cells were serum starved overnight by replacing the growth medium with Clonetics endothelial cell basal medium containing 0.1% bovine serum albumin and 500 μg/mL hydrocortisone. Cells were treated with pazopanib at various concentrations for 1 h followed by addition of 10 ng/mL VEGF or vehicle for 10 min. Cells were solubilized in lysis buffer. VEGFR2 was immunoprecipitated with anti-Flk-1 antibody and analyzed by SDS-PAGE followed by Western blotting and detection with anti-Flk-1 or anti-phosphotyrosine (anti-p-Tyr-biotin) antibody. The VEGFR2 phosphorylation level was quantified by densitometry and normalized to the total VEGFR2 level. For VEGFR2 phosphorylation *in vivo*, female Swiss nude mice were treated with a single p.o. dose of pazopanib before administration of VEGF<sub>121</sub> i.v. (15 μg/mouse). Five minutes after VEGF injection, mice were killed and their lungs were excised and snap frozen. Blood was collected for analysis of pazopanib levels in plasma. Frozen tissue was subsequently homogenized in lysis buffer and VEGFR2 phosphorylation was analyzed as described above.

A similar procedure was used to assess phosphorylation of c-Kit and PDGFRβ using NCI-H526 and human foreskin fibroblast cells, respectively. Cells ( $3 \times 10^6$  per 10-cm dish) were serum starved overnight and treated with pazopanib for 1 h at 37°C before stimulation with 100 ng/mL stem cell factor or 30 ng/mL PDGF-BB. Lysates were prepared, c-Kit

or PDGFRβ was immunoprecipitated, and immunoblots were probed with total receptor or with anti-p-Tyr antibody to reveal the status of c-Kit and PDGFRβ activation after treatment.

#### Tumor Xenografts

Tumors were initiated by injection of tumor cell suspension (HT29, A375P, PC3, and Caki-2) or tumor fragments (BT474 and NCI-H322) s.c. in 8- to 12-week-old nude mice, except PC3 and BT474 tumors, which were grown in severe combined immunodeficient mice (Charles River Laboratories). When tumors reached a volume of 100 to 200 mm<sup>3</sup>, mice were randomized and divided into groups of eight. Pazopanib (using either the di-HCl salt or the mono-HCl salt) was administered once or twice daily at 10, 30, or 100 mg/kg. Animals were euthanized by inhalation of CO<sub>2</sub> at the completion of the study. Tumor volume was measured twice weekly by calipers using the following equation: tumor volume (mm<sup>3</sup>) = (length × width<sup>2</sup>) / 2. Results were routinely reported as % inhibition = 1 - (average growth of the drug-treated population / average growth of vehicle-treated control population).

A similar procedure was used to assess the effect of p.o. dosing versus continuous infusion of a VEGFR inhibitor on HT29 tumor growth. In this study, the VEGFR inhibitor GW771806, which has similar enzyme and cellular profiles to pazopanib (see Supplementary Tables S1A and B),<sup>1</sup> was used. The VEGFR inhibitor was administered by oral gavage at dosages of 100, 30, 10, or 3 mg/kg twice daily or delivered continuously (1 μL/h, 7-day release) via s.c. implanted Alzet osmotic minipump (model #2001, Alzet Osmotic Pumps Company) at a dose of 10, 3, or 1 mg/kg/d.

#### Matrigel Plug Assay

The bFGF/Matrigel angiogenesis assay was modified from the model described by Passaniti et al. (16). Female Swiss *nu/nu* mice were dosed p.o. once or twice on day 0 through day 4 with pazopanib (100, 30, or 10 mg/kg) or vehicle. On day 0, a maximum of 1 h after compound administration, the anesthetized mice were injected s.c. at the ventral midline with 0.5-mL Matrigel (BD Biosciences) containing either 1 μg/mL bFGF or 0.05% bovine serum albumin. On day 5, mice were euthanized and the Matrigel implants were excised and homogenized. Supernatants from homogenized samples were evaluated for angiogenic response by quantitative hemoglobin (Hb) analysis using the Sigma 527-A Plasma hemoglobin assay. Hemoglobin values obtained via colorimetric assay were used to measure efficacy by defining percent inhibition as  $1 - [(Hb_{\text{inhibitor-treated sample}} - Hb_{\text{negative control}}) / (Hb_{\text{positive control}} - Hb_{\text{negative control}})] \times 100$ . A two-tailed Student's *t* test was used to show statistical significance. Hemoglobin end points were used to determine percent of control for each sample. The ED<sub>50</sub> for each dosing regimen was calculated from percent control values using the following formula:  $y = [V_{\max} / 1 + (x / IC_{50})]$ .

Using a similar procedure, the effects of p.o. dosing versus continuous infusion of the VEGFR inhibitor

**Table 1. The IC<sub>50</sub> of pazopanib against the indicated enzyme in a cell-free assay system**

Enzyme	Kinase IC <sub>50</sub> (μmol/L)
VEGFR1	0.010
VEGFR2	0.030
VEGFR3	0.047
PDGFRα	0.071
PDGFRβ	0.084
c-Kit	0.074
FGFR1	0.14
FGFR3	0.13
FGFR4	0.8
c-fms	0.146
LCK	0.411
ITK	0.430
FAK	0.8
p38α	1.056
Abl1	2
JNK1	2.466
Ret	2.8
Src	3.090
GSK3	3.460
JNK3	4.065
ALK6	4.266
Tie-2	4.520
Met	6
IGF-IR	8
JNK2	10.233
Akt3; CDK1 and CDK2; EphB4; ErbB1, ErbB2, and ErbB4; Flt-3; INS-R; PLK1 and PLK3; PKC-β1 and PKC-β2; Syk; Wee1	>20

Abbreviations: LCK, lymphocyte-specific protein tyrosine kinase; ITK, interleukin-2-inducible T-cell kinase; FAK, focal adhesion kinase; JNK1, JNK2, and JNK3, c-jun NH<sub>2</sub>-terminal kinases 1, 2, and 3; GSK3, glycogen synthase kinase 3; ALK6, activin-like kinase 6; IGF-IR, insulin-like growth factor type I receptor; CDK1 and CDK2, cyclin-dependent kinases 1 and 2; INS-R, insulin receptor; PLK1 and PLK3, polo-like kinases 1 and 3; PKC-β1 and PKC-β2, protein kinase C-β1 and -β2.

GW771806 on angiogenesis were studied. Bolus p.o. doses of the VEGFR inhibitor at 10, 30, or 100 mg/kg either once or twice daily on days 0 through 4 were administered. For continuous infusion, GW771806 was administered at doses of 0.3, 1.0, 3.0, or 10 mg/kg per 24 h on days -1 through 5 via s.c. implanted Alzet osmotic minipumps.

#### Mouse Corneal Micropocket Assay

The mouse corneal micropocket assay was conducted to assess the activity of pazopanib against VEGF- and bFGF-induced angiogenesis in female *nu/nu* mice as described earlier (17). On day 0, sucralate-hydrone pellets containing sterile distilled water, 100 ng VEGF, or 80 ng bFGF were implanted under Avertin anesthesia into a pocket created in the cornea, 1 mm from the cornea-limbus interface. Mice were treated with pazopanib at 100 mg/kg, twice daily, by oral gavage on day -2 through day 5. On day 5, the angiogenic response was evaluated by determining the clock

hour and maximum vessel length under stereomicroscope. The magnitude of blood vessel growth along the periphery of the cornea that advances from the vascular limbus and is directed toward the growth factor implant was measured using clock hours. Maximum vessel length was measured in millimeters. The percent inhibition was calculated as follows: % inhibition =  $1 - [(X_{\text{treated sample}} - X_{\text{negative control}}) / (X_{\text{positive control}} - X_{\text{negative control}})] \times 100$ , where  $X$  is clock hours or maximum vessel length. Analysis was done using a two-tailed  $t$  test, assuming unequal variance.

#### Plasma Sample Analysis for Pazopanib and GW771806

Duplicate plasma samples containing pazopanib and GW771806, standards, and quality control samples were precipitated with acetonitrile-containing internal standard (analogues of pazopanib and GW771806). For pazopanib, the resulting supernatant was injected into a dual column TurbulentFlow high-performance liquid chromatography-tandem mass spectrometry system. The chromatography was carried out using two Hewlett Packard 1100 binary pumps, a Cohesive Technologies 2300 switching valve module, and CTC HTS PAS autosampler. Two high-performance liquid chromatography columns were used; the first was a Cohesive Technologies Polar Plus extraction column and the second was a Waters Symmetry Shield RP8 analytic column. The mobile phase system for both columns consisted of 5 mmol/L ammonium acetate (unadjusted pH) and acetonitrile delivered in a gradient run. A Perkin-Elmer Sciex API 300 triple quadrupole mass spectrometer equipped with a turbo ion spray source in the positive ion mode was used to analyze the samples. Analytes were detected by multiple reaction monitoring of the transitions  $m/z$  438 to 357 (pazopanib) and  $m/z$  424 to 343 (internal standard).

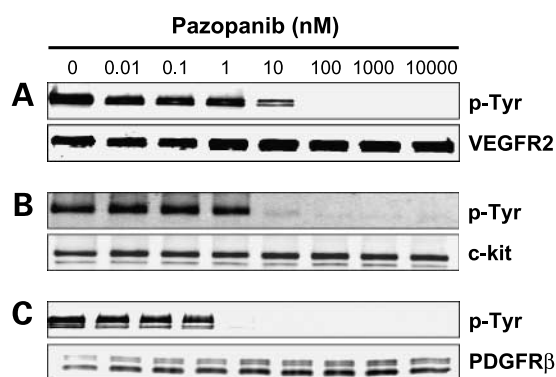


**Figure 1.** Pazopanib inhibits tyrosine autophosphorylation of VEGFR2, c-Kit, and PDGFRβ in cells. Dose response effect of pazopanib was evaluated in ligand-induced autophosphorylation of VEGFR2 in HUVEC (A), c-Kit in NCI-H526 tumor cells (B), and PDGFRβ in human foreskin fibroblasts (C). Cells were treated with different concentrations of pazopanib for 1 h followed by stimulation with 10 ng/mL VEGF (A), 100 ng/mL stem cell factor (B), or 30 ng/mL PDGF-BB (C). Cell lysates were immunoprecipitated with antibodies against total receptor and the samples were analyzed by Western blotting for phosphorylated receptors with anti-p-Tyr antibody. Membranes were stripped and reprobed with anti-receptor antibody to show equal loading.

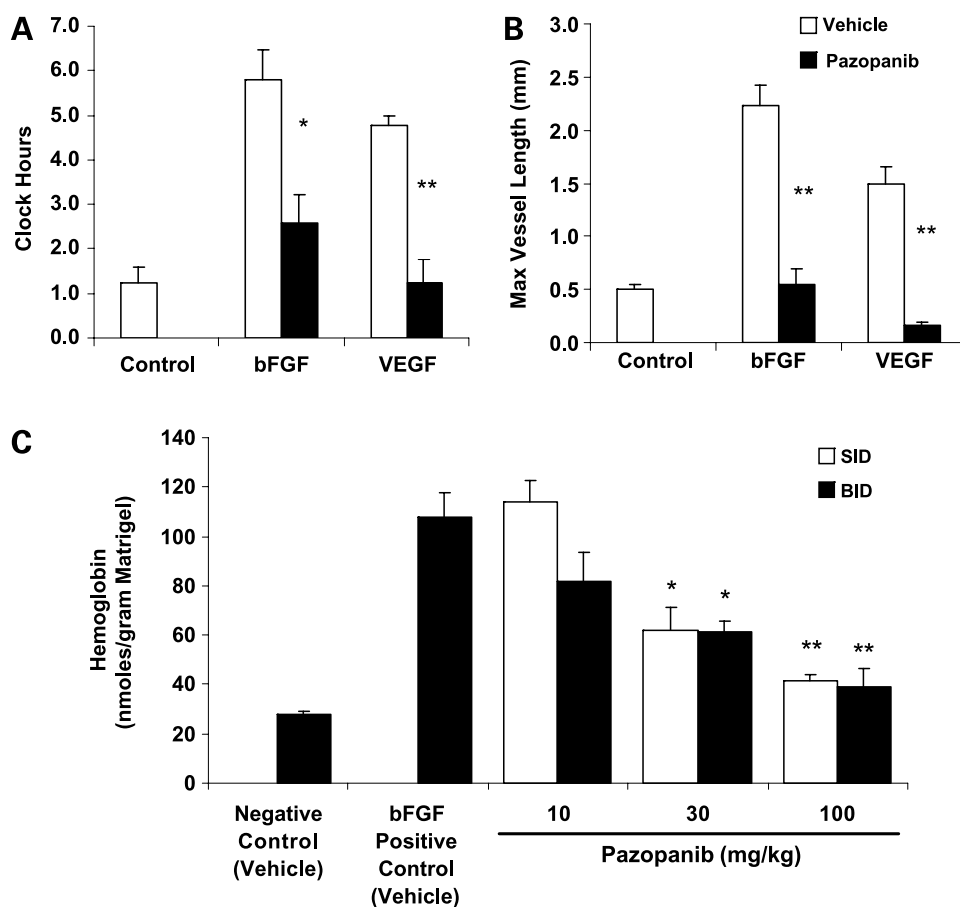


**Figure 2.** Pazopanib inhibits angiogenesis in mouse models. **A** and **B**, angiogenesis was induced by implanting slow release pellets containing either bFGF or VEGF in the mouse cornea. Pazopanib was given p.o. at 100 mg/kg twice daily for 5 d. On day 5 after implantation, the angiogenic response was measured by determining the periphery of the cornea with blood vessels (clock hours) as well as maximal vessel length in each eye. **Columns**, mean from five or more animals in each group; **bars**, SE. \*,  $P < 0.01$ ; \*\*,  $P < 0.001$ , significantly different from vehicle-treated group. **C**, bFGF-containing Matrigel was implanted s.c. in nude mice to induce angiogenesis. On day 5 after implantation, the angiogenic response was measured by determining the hemoglobin content as a surrogate for vascular volume. Pazopanib was given p.o. at 10, 30, or 100 mg/kg once daily (SID) or twice daily (BID) for 5 d. **Columns**, mean from five or more animals in each group; **bars**, SE. \*,  $P < 0.01$ ; \*\*,  $P < 0.001$ , significantly different from bFGF-positive control.

For GW771806, the samples were analyzed on a Hewlett Packard 1100 high-performance liquid chromatography system and a Perkin-Elmer Sciex API 100 mass spectrometer. Samples were injected onto a Phenomenex Luna C18 column. The mobile phase consisted of 13 mmol/L ammonium formate (pH 3.5) with 5% acetonitrile and methanol delivered in a gradient run. Ionization was in the positive mode using electrospray. Analytes of GW771806 and internal standard were detected by single ion monitoring at  $m/z$  437 and  $m/z$  453, respectively. Pazopanib and GW771806 concentrations in plasma were determined by reference to calibration curves constructed by linear regression analysis of  $1/x^2$  weighted peak areas with a correlation coefficient of 0.997.

## Results

### Kinase Activity of Pazopanib

The chemical structure of pazopanib is shown in Supplementary Table S1.<sup>1</sup> Pazopanib is an orally bioavailable, ATP-competitive inhibitor of human VEGFR2 tyrosine kinase ( $K_i = 24 \pm 4$  nmol/L) in an *in vitro* assay. It also inhibits activity of VEGFR2 kinase from dog, mouse, and rat with potencies similar to human VEGFR2 (Supplementary Table S1).<sup>1</sup> Pazopanib inhibits other members of the VEGFR kinase family, including VEGFR1, VEGFR2, and VEGFR3,

and shows similar activity against PDGFR $\alpha$ , PDGFR $\beta$ , and c-Kit (Table 1). It has modest activity against FGFR1, FGFR3, and c-fms receptor tyrosine kinases. Pazopanib was quite selective against a wide panel of kinase evaluated (Table 1). Pazopanib was also evaluated in an Upstate kinase panel of 225 unique kinases at 0.3 and 10  $\mu$ mol/L concentrations in an activity assay. Besides the kinases mentioned above, pazopanib inhibited 13 additional kinases by >50% at 0.3  $\mu$ mol/L. Follow-up studies to evaluate the  $IC_{50}$  of pazopanib against these kinases showed that only 5 of the 13 kinases (Aurora-A, c-Raf, MLK1, PTK5, and TAO3) had  $IC_{50}$ s within 10-fold of VEGFR2 activity. Taken together, these results show that pazopanib is a highly selective kinase inhibitor with potent activity against VEGFR, PDGFR, and c-Kit tyrosine kinases.

### Cellular Activity of Pazopanib

To confirm the measured biochemical activity of pazopanib in a cell-based assay, ligand-induced autophosphorylation of VEGFR2, c-Kit, and PDGFR $\beta$  was evaluated in the presence of pazopanib in cells expressing physiologic levels of the respective receptors. Pazopanib potently inhibited VEGF-induced phosphorylation of VEGFR2 in HUVEC with an  $IC_{50}$  of  $\sim 8$  nmol/L (Fig. 1A). Similarly, pazopanib showed potent inhibition of stem cell factor- and PDGF-BB-induced phosphorylation of c-Kit and

PDGFR $\beta$  in NCI-H526 tumor cells and human foreskin fibroblasts, respectively (Fig. 1B and C). Pazopanib selectively inhibited VEGF-induced proliferation of HUVEC ( $IC_{50} = 21.3 \pm 4.5$  nmol/L) compared with bFGF-induced HUVEC proliferation ( $IC_{50} = 720.9 \pm 239.5$  nmol/L). Pazopanib had no effect on the proliferation of a wide array of tumor cells tested *in vitro* ( $IC_{50} > 10$   $\mu$ mol/L).

#### Pazopanib Inhibits VEGF- and bFGF-Induced Angiogenesis in Mouse Corneal Micropocket and Matrigel Plug Assays

The effect of pazopanib on animal models of angiogenesis was evaluated using two mouse models. In the corneal micropocket assay, ocular angiogenesis was induced by implantation of slow-release pellets containing fixed amounts of VEGF or bFGF into the mouse cornea (17). Five days after implantation, the degree of vascularity was measured in clock hours and maximal vessel length. Vehicle-treated mice show a robust angiogenesis induction with both bFGF and VEGF (Fig. 2A and B). Treatment of mice with 100 mg/kg pazopanib, twice daily, resulted in significant inhibition of both bFGF and VEGF-induced angiogenesis, although the inhibition was more pronounced when VEGF was used as the stimulant.

Pazopanib was also evaluated in a Matrigel plug assay (16) in which angiogenesis was induced by implanting bFGF-containing Matrigel plug under mouse skin. bFGF was used as the angiogenic factor in this model due to the robust angiogenesis induced by FGF compared with recombinant VEGF in this model and the fact that bFGF induces VEGF production in endothelial and other stromal cells (18) and that anti-VEGF antibody can block angiogenesis induced by bFGF in the Matrigel plug assay (data not shown). bFGF-containing Matrigel plug showed robust angiogenesis, as measured by hemoglobin content, compared with negative control Matrigel plug (Fig. 2C). Treatment of mice with pazopanib showed a dose-dependent inhibition of bFGF-induced angiogenesis with >80% inhibition at 100 mg/kg dose given once or twice daily. The  $ED_{50}$  for the once daily dosage regimen was  $29.4 \pm 7.9$  mg/kg and the  $ED_{50}$  for twice daily dosing was  $20.3 \pm 11.3$  mg/kg.

#### Pazopanib Inhibits Growth of Human Tumor Xenografts in Mice

The antitumor activity of pazopanib was evaluated in several human tumor xenograft models in immunocompromised mice. Mice with established tumors (100–250 mm<sup>3</sup>)

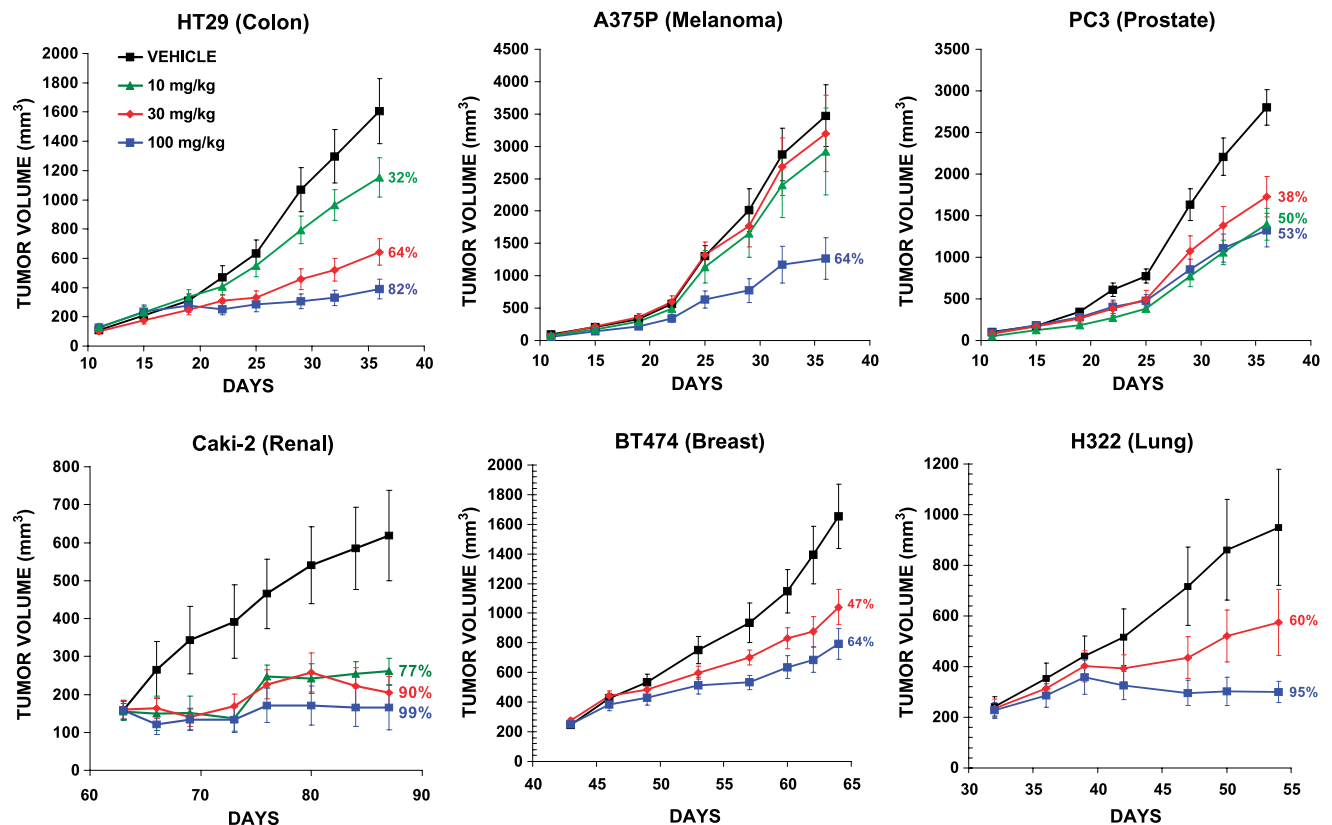


**Figure 3.** Pazopanib has broad antitumor activity. Dose response of pazopanib against established human tumor xenografts in immunocompromised mice. Pazopanib was given p.o. twice daily at 10, 30, and 100 mg/kg to mice bearing HT29 (colon carcinoma), A375P (melanoma), and PC3 (prostate carcinoma) or once daily at 10, 30, or 100 mg/kg to mice bearing Caki-2 (renal carcinoma), BT474 (breast carcinoma), and NCI-H322 (non-small-cell lung carcinoma). Tumor growth inhibition at the end of 21 d of dosing was calculated at various pazopanib doses compared with vehicle-treated mice. Points, mean ( $n = 8$  mice per group); bars, SE.

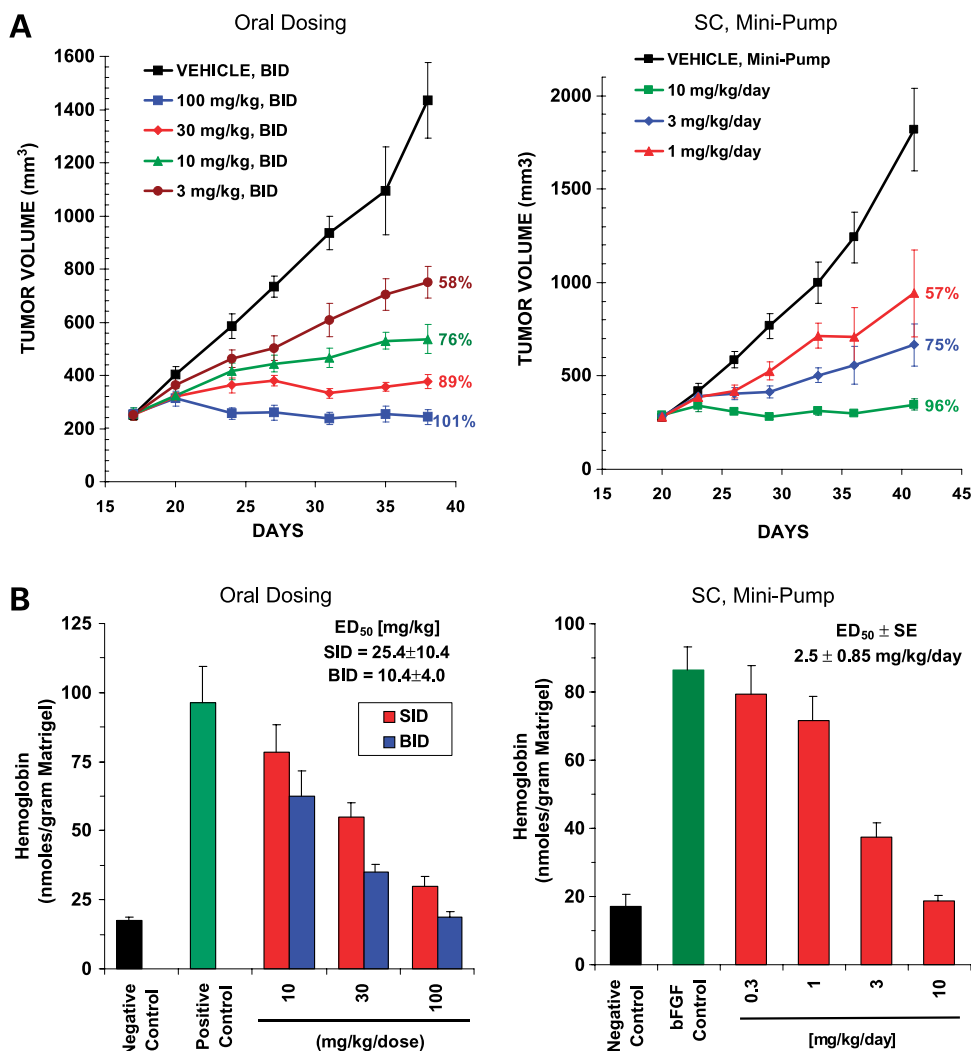


**Figure 4.** Continuous infusion of VEGFR inhibitor is more effective in controlling tumor growth and angiogenesis than p.o. bolus dosing. **A**, nude mice bearing established HT29 tumor xenografts were treated with various doses of GW771806 given p.o. at twice daily schedule for 21 d (left) or via continuous infusion using osmotic mini-pumps for 21 d (right). Tumor growth inhibition at the end of 21 d of dosing was calculated at various pazopanib doses compared with vehicle-treated mice. Points, mean ( $n = 8$  mice per group); bars, SE. **B**, bFGF-containing Matrigel was implanted s.c. in nude mice to induce angiogenesis. GW771806 was administered either p.o. at once or twice daily schedule (left) or via continuous infusion using osmotic mini-pumps (right) for 5 d. On day 5 after implantation, the angiogenic response was measured by determining the hemoglobin content. Columns, mean ( $n = 8$  mice per group); bars, SE.

were randomized in groups of eight animals and treated with vehicle or 10, 30, or 100 mg/kg of pazopanib given once daily (Caki-2, BT474, and NCI-H322) or twice daily (HT29, A375P, and PC3) by oral gavage for 21 days. Once or twice daily treatment with pazopanib at the doses used had no significant effect on the body weight of mice and the animal appeared healthy and active throughout the study duration. Pazopanib showed a dose-dependent growth inhibition of all the tumor xenografts tested (Fig. 3), although the degree of inhibition varied among different models. Caki-2, a renal cell carcinoma, was most sensitive to pazopanib with 77% inhibition at 10 mg/kg dose and complete cytostasis in mice treated with 100 mg/kg dose. HT29, colon carcinoma, and NCI-H322 (non-small-cell lung carcinoma) also showed almost complete inhibition of tumor growth in mice treated with 100 mg/kg pazopanib. A375P (melanoma), PC3 (prostate carcinoma), and BT474 (breast carcinoma) showed a more modest inhibition of tumor growth with maximal inhibition reaching 53% to 64% at 100 mg/kg dose. Continued daily treatment was required for maximal antitumor activity with pazopanib in mouse models.

#### ***In vivo* Activity of VEGFR Inhibitor Is Determined by Steady-State Plasma Concentration *In vivo***

To better understand the relationship of various pharmacokinetic variables with *in vivo* antitumor and antiangiogenic activities, drug administration by bolus p.o. dosing and continuous infusion using s.c. Alzet osmotic pumps were evaluated in the HT29 tumor xenograft model and Matrigel plug assays. For these studies, GW771806 was used due to the limited solubility of pazopanib for continuous infusion studies. GW771806 is a close analogue of pazopanib with similar kinase and cellular activities (Supplementary Tables S1 and S2).<sup>1</sup> In the HT29 tumor xenograft model, p.o. dosing of GW771806 resulted in 58%, 76%, 89%, and 101% inhibition of tumor growth at 3, 10, 30, and 100 mg/kg, twice daily schedule (Fig. 4A). Continuous infusion of GW771806 at 1, 3, and 10 mg/kg/d caused inhibition of HT29 tumor growth by 57%, 75%, and 96%, respectively, compared with vehicle-treated mice. The steady-state concentration of GW771806 at the end of 21 days of dosing in mice with continuous infusion were 0.26, 0.73, and 2.57  $\mu\text{mol/L}$  in mice receiving 1, 3, and 10 mg/kg/d,

respectively. Single p.o. administration of GW771806 resulted in  $C_{max}$  of 21.6, 26.6, and 37.7  $\mu\text{mol/L}$  at 10, 30, and 100 mg/kg doses (Supplementary Fig. S1 and Table S3).<sup>1</sup> These data clearly showed that  $C_{max}$  is not a good indicator of antitumor activity because 2.57  $\mu\text{mol/L}$  constant plasma concentration of GW771806 with continuous infusion was more effective than  $>20 \mu\text{mol/L}$   $C_{max}$  achieved with 10 and 30 mg/kg p.o. dosing.

The effect of p.o. dosing versus continuous infusion was also compared in the bFGF-induced Matrigel plug assay. GW771806 was administered p.o. at 10, 30, and 100 mg/kg doses, once or twice daily, or by continuous infusion using Alzet osmotic pumps at 0.3, 1, 3, and 10 mg/kg/d for 5 days. GW771806 showed a dose-dependent inhibition of angiogenesis when given p.o. with  $ED_{50}$  values of 25.4 and 20.8 mg/kg/d with once or twice daily dosing schedule, respectively (Fig. 4B). When GW771806 was given by continuous infusion, a dose-dependent inhibition of angiogenesis was also observed with an  $ED_{50}$  value of 2.5 mg/kg/d. Plasma concentrations of GW771806 were collected on day 2 of dosing in a parallel cohort of mice with osmotic pumps. The GW771806 concentrations in this study were similar to those observed in the HT29 tumor xenograft study with a steady-state concentration of 0.09, 0.23, 0.65, and 2.67  $\mu\text{mol/L}$  at 0.3, 1, 3, and 10 mg/kg/d, respectively. A steady-state plasma concentration of 2.67  $\mu\text{mol/L}$  at 10 mg/kg/d showed complete inhibition of angiogenesis in the Matrigel plug assay, suggesting that both HT29 tumor growth and angiogenesis are not driven by the  $C_{max}$  of the VEGFR inhibitor.

#### Steady-State Plasma Concentration Required for *In vivo* Efficacy Is Consistent with the Concentration Required for the Inhibition of VEGFR2 Phosphorylation *In vivo*

Due to their high endothelial cell content, the effect of VEGFR inhibitors on VEGF-induced VEGFR2 phosphorylation was evaluated in mouse lungs. GW771806 inhibited VEGF-induced VEGFR2 phosphorylation in murine lungs in a dose- and time-dependent manner (Fig. 5A and B). VEGFR2 phosphorylation was inhibited in this model at 1 h after a single p.o. dose of GW771806 at  $\geq 1$  mg/kg. A time course study showed almost complete inhibition of VEGFR2 phosphorylation for up to 8 h after a single p.o. dose of 10 mg/kg GW771806. Plasma concentration analysis at the time of lung harvesting suggests that  $\sim 1$  to 2  $\mu\text{mol/L}$  of GW771806 is required for optimal inhibition of VEGFR2 phosphorylation in mice. These results are in agreement with the inhibition of angiogenesis in the Matrigel plug assay and inhibition of HT29 tumor xenograft growth using continuous delivery of GW771806, in which maintaining a steady-state plasma concentration of  $\geq 2.5 \mu\text{mol/L}$  GW771806 resulted in  $>90\%$  inhibition of angiogenesis as well as HT29 tumor growth.

#### Plasma Concentration of $\sim 40 \mu\text{mol/L}$ Pazopanib Is Required for Maximal Inhibition of VEGFR2 Phosphorylation in Mice

To determine the steady-state concentration required for *in vivo* activity of pazopanib, VEGF-induced VEGFR2

phosphorylation in mouse lungs was assessed after p.o. dosing with pazopanib. A single p.o. dose of 30 mg/kg pazopanib inhibited phosphorylation for  $>8$  h corresponding to  $>40 \mu\text{mol/L}$  plasma concentration (Fig. 5C). Mean plasma concentrations of 153.9, 47.5, 41.1, 17.4, and 4.3  $\mu\text{mol/L}$  were achieved at 1, 4, 8, 16, and 24 h, respectively. At 16 and 24 h, the plasma concentration dropped below 40  $\mu\text{mol/L}$  and the inhibition of VEGFR2 phosphorylation was minimal, if any. These results, together with those observed with GW771806, show that a steady-state concentration of  $\geq 40 \mu\text{mol/L}$  pazopanib is required for optimal *in vivo* activity.

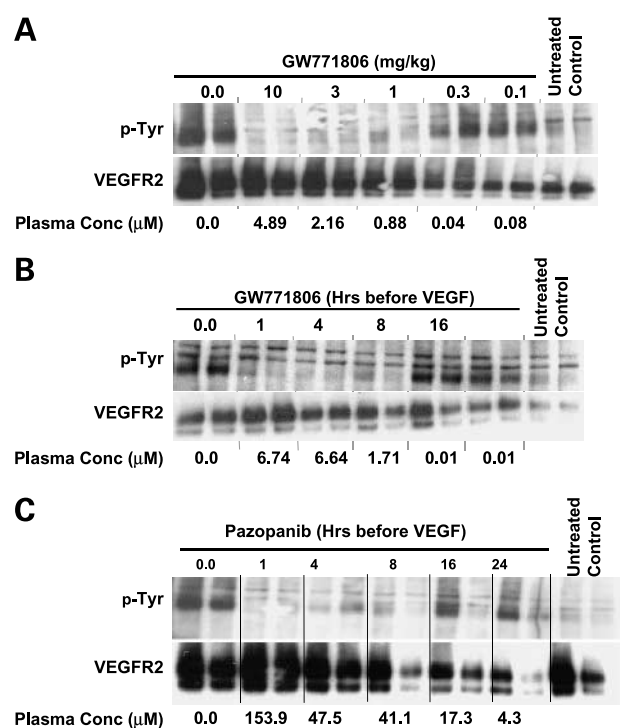


**Figure 5.** GW771806 and pazopanib inhibit VEGFR2 phosphorylation *in vivo*. **A**, mice were given a single p.o. dose of GW771806 at 0.1, 0.3, 1, 3, and 10 mg/kg. One hour later, VEGF (15  $\mu\text{g}/\text{mouse}$ ) was administered by tail vein injection and lungs were collected 5 min afterwards. Lysates were immunoprecipitated with anti-VEGFR2 antibody and analyzed by Western blotting for phosphorylated and total receptors. Plasma concentration of GW771806 was evaluated in corresponding mice at the time of tissue collection. Each lane represents sample from a separate mouse. GW771806 concentration is mean of two mice at each dose level. **B**, time course of VEGFR2 inhibition *in vivo* after single p.o. dose of 10 mg/kg GW771806. VEGF was administered by tail vein injection at 1, 4, 8, 16, and 24 h after GW771806 dosing. Phosphorylated and total VEGFR2 were analyzed by immunoprecipitation and Western blotting. Each lane represents sample from a separate mouse. GW771806 concentration is mean of two mice at each dose level. **C**, time course of VEGFR2 inhibition *in vivo* after single p.o. dose of pazopanib. VEGF (15  $\mu\text{g}/\text{mouse}$ ) was administered by tail vein injection at 1, 4, 8, 16, and 24 h after pazopanib (30 mg/kg) dosing. Phosphorylated and total VEGFR2 were analyzed by immunoprecipitation and Western blotting. Each lane represents sample from a separate mouse. Pazopanib concentration is mean of two mice at each dose level.



## Discussion

Whereas angiogenesis presents many potential therapeutic targets, the VEGFR2 signal pathway has emerged as a primary paracrine/autocrine regulator of endothelial cell biology (18–20). Preclinical studies show that pazopanib is a potent inhibitor of all three VEGF receptors *in vitro* and that it inhibits HUVEC proliferation in response to VEGF. Although pazopanib is >30-fold selective for VEGF-induced endothelial cell proliferation compared with that induced by bFGF, it inhibits both VEGF- and bFGF-mediated angiogenesis *in vivo*. This apparent paradox can be explained by earlier observations that bFGF induces VEGF production in endothelial and other stromal cells (18) and that anti-VEGF antibody can block angiogenesis induced by bFGF in the Matrigel plug assay (data not shown). Pazopanib inhibits the growth of a broad range of human tumor xenografts in mice, and a single p.o. dose of 30 mg/kg inhibits VEGF-induced VEGFR2 phosphorylation *in vivo*.

We hoped to use data obtained from preclinical studies to determine the optimal pazopanib drug concentration required for *in vivo* antitumor/antiangiogenic activity. To determine if  $C_{\text{steady-state}}$  or  $C_{\text{max}}$  was the primary determinant of activity, we compared the data from bolus dose administration with those obtained from continuous s.c. infusion administration. These studies were attempted with pazopanib, but because of its poor solubility, we were unable to achieve a high enough drug concentration during parenteral administration. Therefore, a related compound, GW771806, was used to evaluate the importance of  $C_{\text{steady-state}}$  and  $C_{\text{max}}$  values. This molecule has similar enzyme and cellular activity to pazopanib but has different pharmacokinetics after p.o. dosing in mice. GW771806 was discontinued in favor of pazopanib due to overall better developability profile of pazopanib (lower clearance across multiple species). GW771806 was evaluated in antitumor (HT29) and antiangiogenic (Matrigel plug) assays at different doses administered by bolus p.o. route or via continuous infusion. Constant infusion of the compound resulted in an 8- to 10-fold lower  $ED_{50}$  relative to bolus administration, leading us to compare various pharmacokinetic variables with observed *in vivo* activity.  $C_{\text{max}}$  and exposure (AUC) did not correlate with activity, whereas  $C_{\text{steady-state}}$  from bolus and continuous dosing showed overlapping activity.  $C_{\text{steady-state}}$  ( $C_{12\text{ h}}$ ) for twice daily p.o. dosing was similar to that obtained with continuous infusion, and the inhibition of angiogenesis observed in the Matrigel plug assay was also similar (Fig. 4B; Supplementary Fig. S2 and Table S4). Similarly,  $C_{\text{steady-state}}$  correlated with inhibition of HT29 tumor growth as well (Fig. 4A). Furthermore,  $C_{\text{steady-state}}$  achieved in the Matrigel plug assay and HT29 antitumor study with 10 mg/kg/24 h were  $\sim 2.5$   $\mu\text{mol/L}$  GW771806, which were close to the drug concentration required for inhibition of VEGF-induced VEGFR2 phosphorylation *in vivo* (Fig. 5). We were not able to detect VEGFR2 phosphorylation in tumor xenografts due to low endothelial cell content, but because endothelial cells in both xenografts and naïve

lungs were of mouse origin, the concentration required to inhibit VEGFR2 phosphorylation should be similar in both tissues. These results clearly show that steady-state plasma concentration required for *in vivo* efficacy is consistent with the concentration required for the inhibition of VEGFR2 phosphorylation *in vivo* and that the drug concentration required for VEGFR2 inhibition can be used to predict pharmacokinetic requirements for VEGFR2 inhibitors.

Pharmacokinetic/pharmacodynamic studies showed that a pazopanib concentration of  $\geq 40$   $\mu\text{mol/L}$  is required for inhibition of VEGFR2 in mice. These data differed from the  $IC_{50}$  of 0.02  $\mu\text{mol/L}$  based on VEGF-stimulated proliferation of HUVEC. The discrepancy between *in vivo* and *in vitro* requirements can be attributed to >99.9% protein binding for pazopanib.

A phase I dose escalation study of pazopanib in cancer patients applied these preclinical findings to dosage selection. A target steady-state concentration of  $\geq 40$   $\mu\text{mol/L}$  was selected after once daily dosing based on concentrations required for optimal antitumor and antiangiogenic activity in animals. This steady-state concentration was achieved in the majority of patients receiving doses of  $\geq 800$  mg once daily or 300 mg twice daily (11). A decrease in tumor perfusion as measured by dynamic contrast enhanced magnetic resonance imaging was observed in patients receiving 800 mg once daily or 300 mg twice daily dose. Hypertension seems to be a class effect of all VEGF signaling inhibitors in the clinic (21) and can be used as a potential pharmacodynamic marker for inhibition of VEGF signaling. There seemed to be a correlation between hypertension and steady-state concentration in phase I study of pazopanib, with 53% of patients achieving  $C_{\text{steady-state}} > 46$   $\mu\text{mol/L}$  (20  $\mu\text{g/mL}$ ) showing an increase in blood pressure whereas only 18% of patients with  $C_{\text{steady-state}} < 46$   $\mu\text{mol/L}$  had an increase in blood pressure. Further evidence of clinical activity, including partial responses, was observed in patients dosed at 800 mg once daily or 300 mg twice daily (11). Based on these results, 800 mg once daily dose was used for subsequent phase II single agent studies for pazopanib in patients with diverse tumor types.

In summary, our data show that pazopanib is a potent multikinase inhibitor of VEGFR, PDGFR, and c-Kit receptors with antitumor and antiangiogenic activity *in vivo*. Preclinical pharmacokinetic-pharmacodynamic studies showed requirements of  $\geq 40$   $\mu\text{mol/L}$  plasma concentration for optimal *in vivo* activity. Observed pharmacodynamic effects and antitumor activity in phase I trial with pazopanib show a strong correlation between preclinical and clinical pharmacokinetics-pharmacodynamics. This suggests that preclinical models can be used to guide pharmacokinetic-based dose selection for VEGFR inhibitors in human. Pazopanib is currently being studied in multiple clinical trials as a single agent as well as in combination with various agents.

## References

1. Hanahan D, Weinberg RA. The hallmarks of cancer. *Cell* 2000;100:57–70.

2. Hanahan D, Folkman J. Patterns and emerging mechanisms of the angiogenic switch during tumorigenesis. *Cell* 1996;86:353–64.
3. Berse B, Brown LF, Van de Water L, Dvorak HF, Senger DR. Vascular permeability factor (vascular endothelial growth factor) gene is expressed differently in normal tissues, macrophages, and tumors. *Mol Biol Cell* 1992;3:211–20.
4. Dvorak HF. Vascular permeability factor/vascular endothelial growth factor: a critical cytokine in tumor angiogenesis and a potential target for diagnosis and therapy. *J Clin Oncol* 2002;20:4368–80.
5. Millauer B, Witzigmann-Voos S, Schnürch H, et al. High affinity VEGF binding and developmental expression suggest Flk-1 as a major regulator of vasculogenesis and angiogenesis. *Cell* 1993;72:835–46.
6. Zeng H, Dvorak HF, Mukhopadhyay D. Vascular permeability factor (VPF)/vascular endothelial growth factor (VEGF) receptor-1 down-modulates VPF/VEGF receptor-2-mediated endothelial cell proliferation, but not migration, through phosphatidylinositol 3-kinase-dependent pathways. *J Biol Chem* 2001;276:26969–79.
7. Song S, Ewald AJ, Stallcup W, Werb Z, Bergers G. PDGFR $\beta$ <sup>+</sup> perivascular progenitor cells in tumours regulate pericyte differentiation and vascular survival. *Nat Cell Biol* 2005;7:870–9.
8. Östman A. PDGF receptors—mediators of autocrine tumor growth and regulators of tumor vasculature and stroma. *Cytokine Growth Factor Rev* 2004;15:275–86.
9. Lennartsson J, Rönstrand L. The stem cell factor receptor/c-Kit as a drug target in cancer. *Curr Cancer Drug Targets* 2006;6:65–75.
10. Morabito A, De Maio E, Di Maio M, Normanno N, Perrone F. Tyrosine kinase inhibitors of vascular endothelial growth factor receptors in clinical trials: current status and future directions. *Oncologist* 2006;11:753–64.
11. Hurwitz H, Dowlati A, Savage S, et al. Safety, tolerability, and pharmacokinetics of oral administration of GW780634 in pts with solid tumors. *J Clin Oncol* 2005;23 Suppl 16S:3012.
12. Sandler AB, Gray R, Brahmer J, et al. Randomized phase II/III Trial of paclitaxel (P) plus carboplatin (C) with or without bevacizumab (NSC # 704865) in patients with advanced non-squamous non-small cell lung cancer (NSCLC): An Eastern Cooperative Oncology Group (ECOG) Trial-E4599. *J Clin Oncol* 2005;23 Suppl 16S:4.
13. Motzer RJ, Michaelson MD, Redman BG, et al. Activity of SU11248, a multitargeted inhibitor of vascular endothelial growth factor receptor and platelet-derived growth factor receptor, in patients with metastatic renal cell carcinoma. *J Clin Oncol* 2006;24:16–24.
14. Demetri GD, van Oosterom AT, Garrett CR, et al. Efficacy and safety of sunitinib in patients with advanced gastrointestinal stromal tumor after failure of imatinib; a randomised controlled trial. *Lancet* 2006;368:1329–38.
15. Ratain MJ, Eisner T, Stadler WM, et al. Phase II placebo-controlled randomized discontinuation trial of Sorafenib in patients with metastatic renal cell carcinoma. *J Clin Oncol* 2006;24:2505–12.
16. Passaniti A, Taylor RM, Pili R, et al. A simple, quantitative method for assessing angiogenesis and antiangiogenic agents using reconstituted basement membrane, heparin, and fibroblast growth factor. *Lab Invest* 1992;67:519–28.
17. Kenyon BM, Voest EE, Chen CC, Flynn E, Folkman J, D'Amato RJ. A model of angiogenesis in the mouse cornea. *Invest Ophthalmol Vis Sci* 1996;37:1625–32.
18. Seghezzi G, Patel S, Ren CJ, et al. Fibroblast growth factor-2 (FGF-2) induces vascular endothelial growth factor (VEGF) expression in the endothelial cells of forming capillaries: an autocrine mechanism contributing to angiogenesis. *J Cell Biol* 1998;141:1659–73.
19. Shifren JL, Doldi N, Ferrara N, Mesiano S, Jaffe RB. In the human fetus, vascular endothelial growth factor is expressed in epithelial cells and myocytes, but not vascular endothelium: implications for mode of action. *J Clin Endocrinol Metab* 1994;79:316–22.
20. Veikkola T, Karkkainen M, Claesson-Welsh L, Alitalo K. Regulation of angiogenesis via vascular endothelial growth factor receptors. *Cancer Res* 2000;60:203–12.
21. Sica DA. Angiogenesis inhibitors and hypertension: an emerging issue. *J Clin Oncol* 2006;24:1329–31.

# Molecular Cancer Therapeutics

## Pharmacokinetic-pharmacodynamic correlation from mouse to human with pazopanib, a multikinase angiogenesis inhibitor with potent antitumor and antiangiogenic activity

Rakesh Kumar, Victoria B. Knick, Sharon K. Rudolph, et al.

*Mol Cancer Ther* 2007;6:2012-2021.

<b>Updated version</b>	Access the most recent version of this article at: <a href="http://mct.aacrjournals.org/content/6/7/2012">http://mct.aacrjournals.org/content/6/7/2012</a>
<b>Supplementary Material</b>	Access the most recent supplemental material at: <a href="http://mct.aacrjournals.org/content/suppl/2007/07/16/6.7.2012.DC1">http://mct.aacrjournals.org/content/suppl/2007/07/16/6.7.2012.DC1</a>

<b>Cited articles</b>	This article cites 21 articles, 10 of which you can access for free at: <a href="http://mct.aacrjournals.org/content/6/7/2012.full#ref-list-1">http://mct.aacrjournals.org/content/6/7/2012.full#ref-list-1</a>
<b>Citing articles</b>	This article has been cited by 46 HighWire-hosted articles. Access the articles at: <a href="http://mct.aacrjournals.org/content/6/7/2012.full#related-urls">http://mct.aacrjournals.org/content/6/7/2012.full#related-urls</a>

<b>E-mail alerts</b>	<a href="#">Sign up to receive free email-alerts</a> related to this article or journal.
<b>Reprints and Subscriptions</b>	To order reprints of this article or to subscribe to the journal, contact the AACR Publications Department at <a href="mailto:pubs@aacr.org">pubs@aacr.org</a> .
<b>Permissions</b>	To request permission to re-use all or part of this article, use this link <a href="http://mct.aacrjournals.org/content/6/7/2012">http://mct.aacrjournals.org/content/6/7/2012</a> . Click on "Request Permissions" which will take you to the Copyright Clearance Center's (CCC) Rightslink site.